Chiral Palladium(II)−Bis(trichlorosilyl) Complexes. Synthesis, Structure, and Combined QM/MM Computational Studies

Tom K. Woo, Giorgio Pioda, Ursula Rothlisberger,* and Antonio Togni*

Laboratory of Inorganic Chemistry, Swiss Federal Institute of Technology, ETH Zentrum, CH-8092 Zürich, Switzerland

Received February 11, 2000

The $PdCl_2$ complexes **1**−**3** (**1**, dichloro{1-{(*R*)-1-[(*S*)-2-(diphenylphosphino-κP)ferrocenyl]-ethyl}-3,5-dimethyl-1*H*-pyrazole-κN}palladium; **2**, dichloro{1-{(*R*)-1-[(*S*)-2-(diphenylphosphino-κP)ferrocenyl]ethyl}-3-phenyl-5-methyl-1*H*-pyrazole-κN}palladium; **3**, dichloro{1-{(*R*)-1-[(*S*)-2-(diphenylphosphino-κP)ferrocenyl]ethyl}-3-(2,4,6-trimethylphenyl)-1*H*-pyrazole-κN}palladium), previously used as catalyst precursors in the asymmetric hydrosilylation of olefins, were found to react with an excess of $HSiCl_3$ in CH_2Cl_2 to afford the corresponding bis(trichlorosilyl) derivatives **4**−**6**, respectively. Two of the new complexes (**5** and **6**) were characterized by X-ray crystallography and revealed unusual structural properties. A severe deviation from the ideal square-planar geometry was observed, as well as extremely elongated Pd−P bonds (Pd−P = 2.4559(16) Å for **5** and 2.504(2) Å for **6**). The nature of the uncommon structural features observed in the bis(trichlorosilyl) derivatives has been explored with density functional theory calculations and the combined quantum mechanics/molecular mechanics (QM/MM) method. Using the combined QM/MM approach a systematic series of model systems have been constructed in which the steric and electronic influences of the substituent groups were selectively removed or altered. The technique has allowed the exact nature of the geometric distortions to be pinpointed.

Introduction

A large number of transition-metal silyl complexes are known, and these species constitute important intermediates in several catalytic reactions involving the hydrosilylation and disilylation of unsaturated functionalities.[1] Characterized compounds include mono-, di-, and polynuclear silyl complexes, most of them formed from alkyl- and/or arylsilanes.[1a] The Pd-catalyzed hydrosilylation with trichlorosilane offers a powerful tool for the "one pot" conversion of an olefin into an alcohol, via the oxidation of the alkyltrichlorosilane intermediate by the method developed by Tamao.[2] It is reasonable to assume that Pd trichlorosilyl complexes participate in the catalytic cycle. However, isolated and characterized species of this kind are still extremely rare.[3] The representative derivative $[(MePh_2P)_2Pd(SiCl_3)_2]$ was obtained by Schubert upon reaction of the corresponding dichloro complex with $HSiCl_3$ in the presence of KH.[3b] The complex was reported to be thermally unstable, and no crystal structure was determined. Furthermore, there appears to be only few Pd(II) *cis*-bis(silyl) complexes that were characterized by X-ray diffraction.[4]

We recently reported that $PdCl_2$ complexes of types **1**−**3** (Chart 1) containing ferrocenyl phosphino pyrazole ligands[5] are suitable catalyst precursors for the highly enantioselective hydrosilylation of norbornene and other olefins with $HSiCl_3$.[6] We now found that such complexes smoothly react with an excess of $HSiCl_3$, leading to the corresponding *cis*-bis(trichlorosilyl) derivatives in crystalline form and in good yields. The present report addresses the structural and spectroscopic characterization of these new and rare derivatives. In comparison to the analogous $PdCl_2$ complexes and other similar

(1) For reviews, see: (a) Corey, J. Y.; Braddock-Wilking, J. *Chem. Rev.* **1999**, *99*, 175−292. (b) Eisen, M. S. In *The Chemistry of Organic Silicon Compounds*; Patai, S., Rappoport, Z., Eds.; Wiley: New York, 1998; Chapter 35. (c) Tilley, T. D. In *The Chemistry of Organic Silicon Compounds* Patai, S., Rappoport, Z., Eds.; Wiley: New York, 1989; Chapter 24. (d) Tilley, T. D. In *The Silicon-Heteroatom Bond*; Patai, S., Rappoport, Z., Eds.; Wiley: Chichester, U.K., 1991; pp 245−359. (e) Gauvin, F.; Harrod, J. F.; Woo, H. G. *Adv. Organomet. Chem.* **1998**, *42*, 363. For recent mechanistic and theoretical works on the hydrosilylation reaction, see: (f) LaPointe, A. M.; Rix, F. C.; Brookhart, M. *J. Am. Chem. Soc.* **1997**, *119*, 906. (g) Bosnich, B. *Acc. Chem. Res.* **1998**, *31*, 667. (h) Sakaki, S.; Mizoe, N.; Sugimoto, M. *Organometallics* **1998**, *17*, 2510.

(2) (a) Tamao, K.; Yoshida, J.; Takahashi, M.; Yamamoto, H.; Kakui, T.; Matsumoto, H.; Kurita, A.; Kumada, M. *J. Am. Chem. Soc.* **1978**, *100*, 290. (b) Tamao, K.; Kakui, T.; Kumada, M. *J. Am. Chem. Soc.* **1978**, *100*, 2268. (c) Tamao, K.; Ishida, N.; Tanaka, T.; Kumada, M. *Organometallics* **1983**, *2*, 1694. See also: (d) Uozumi, Y.; Kitayama, K.; Hayashi, T.; Yanagi, K.; Fukuyo, E. *Bull. Chem. Soc. Jpn.* **1995**, *68*, 713 and references therein.

(3) (a) Eaborn, C.; Griffiths, R. W.; Pidcock, A. *J. Organomet. Chem.* **1982**, *225*, 331. (b) Schubert, U.; Müller, C. *J. Organomet. Chem.* **1989**, *373*, 165.

(4) (a) Pan, Y.; Mague, J. T.; Fink, M. J. *Organometallics* **1992**, *11*, 3495. (b) Suginome, M.; Oike, H.; Park, S.-S.; Ito, Y. *Bull. Chem. Soc. Jpn.* **1996**, *69*, 289. (c) Murakami, M.; Yoshida, T.; Ito, Y. *Organometallics* **1994**, *13*, 2900. (d) Suginome, M.; Oike, H.; Shuff, P. H.; Ito, Y. *Organometallics* **1996**, *15*, 2170. (e) Suginome, M.; Kato, Y.; Takeda, N.; Oike, H.; Ito, Y. *Organometallics* **1998**, *17*, 495.

(5) Burckhardt, U.; Hintermann, L.; Schnyder, A.; Togni, A. *Organometallics* **1995**, *14*, 5415.

(6) (a) Pioda, G.; Togni, A. *Tetrahedron: Asymmetry* **1998**, *9*, 3903. (b) Togni, A.; Dorta, R.; Köllner, C.; Pioda, G. *Pure Appl. Chem.* **1998**, *70*, 1478. (c) Togni, A.; Bieler, N.; Burckhardt, U.; Köllner, C.; Pioda, G.; Schneider, R.; Schnyder, A. *Pure Appl. Chem.* **1999**, *71*, 1531.

10.1021/om000130g CCC: $19.00
Publication on Web 04/29/2000

Chart 1

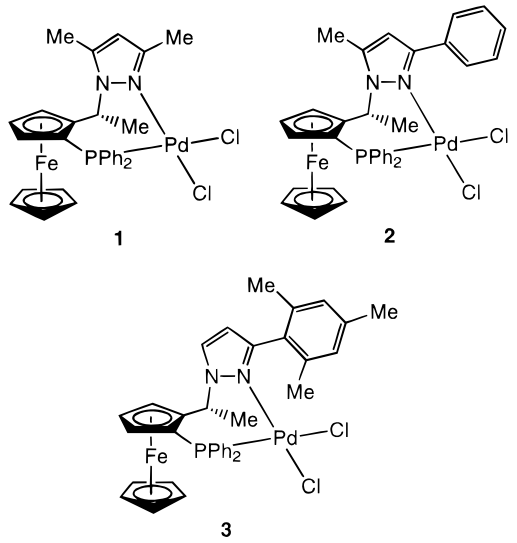

compounds, the bis(trichlorosilyl) derivatives possess some unexpected structural properties, including the longest known Pd−P bond distance of 2.50 Å. To rationalize such unique structural features, the experimental work is complemented by a computational study using state-of-the-art first-principles and combined QM/MM methods. The combined QM/MM method has traditionally been used to perform high-level molecular orbital calculations on extended systems that are too large to be efficiently treated wholly at the quantum-mechanical level. In this work, the combined QM/MM method will be used as a novel analytic tool to probe the steric versus electronic nature of the unexpected structural features observed.

Results and Discussion

Synthesis and Properties in Solution. The dichloro complexes **1**−**3** react with a large excess (ca. 20−30-fold) of $HSiCl_3$ in CH_2Cl_2 at room temperature over a period of ca. 3 days. The corresponding bis(trichlorosilyl) derivatives **4**−**6** (Scheme 1) may be precipitated from the reaction mixture upon addition of hexane and are isolated as air-sensitive yellow powders in 75−84% yield. In the case of **6**, the product crystallizes directly from the reaction mixture. The byproduct HCl does not need to be trapped by a base. The diiodo complex **7**, containing the same ligand as **1**, does not form **4** under the same conditions, and decomposition to palladium black occurs upon heating. Formation of complexes **4**−**6** is likely to follow two consecutive oxidative-addition/reductive-elimination steps, in particular because of the specific ligand combination in the starting materials:[7] they contain only one phosphine donor, and facile dissociation of the pyrazolyl nitrogen is to be assumed (vide infra).[8]

Scheme 1

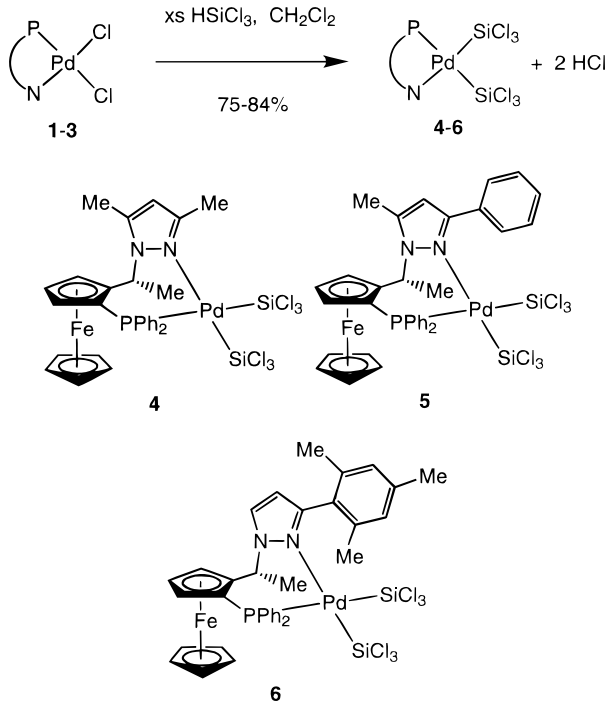

The new silyl complexes are moderately stable, and their stability appears to correlate with the decreasing bulkiness of the P,N-ligand (**4** > **5** > **6**). Thus, complex **4** does not decompose in solution even in the absence of trichlorosilane. On the other hand, **6** is insoluble in CH_2Cl_2, $CHCl_3$, and Et_2O and decomposes in THF and acetone, hence rendering its characterization in solution impossible. ^1H, ^{13}C, and ^{31}P NMR spectra were recorded in CD_2Cl_2 (sealed tube; see Experimental Section) for **4** and **5**. Both compounds show a singlet in the ^{31}P NMR spectrum with one set of ^{29}Si satellites (**4**, δ +6.90 ppm, $^2J(P,Si_{trans})$ = 317 Hz; **5**, δ +6.44 ppm, $^2J(P,Si_{trans})$ = 308 Hz). In both cases no coupling to the silicon in the cis position could be detected. However, the ^{29}Si NMR spectrum of **5** revealed two doublets at 19.3 ppm ($^2J(Si_{trans},P)$ = 308 Hz) and at 14.3 ppm ($^2J(Si_{cis},P)$ = 11 Hz), respectively. The small $^2J(Si_{cis},P)$ coupling constant could not be detected in the ^{29}Si NMR spectrum of **4** (20.4 ppm, $^2J(Si_{trans},P)$ = 317 Hz; 16.4 ppm). The assignment of the two ^{29}Si resonances is based upon the magnitude of the observed coupling and was confirmed by a $^{31}P-^{29}Si\{^1H\}$−HMQC experiment run for **5**, as illustrated in Figure 1.

Solid-State Structure of Complexes 2, 5, and 6. Crystals of derivatives **5** and **6** suitable for an X-ray crystallographic study were obtained from dilute CH_2Cl_2 solutions. Because of the distorted geometry that was found for these two compounds (vide infra), the structure of one of the precursor dichloro complexes (**2**) was also determined for comparison. Table 1 gives the relevant crystal and data collection parameters, and a selection of bond distances and angles, important for the discussion of the coordination sphere of the Pd atoms, is provided in Table 2. ORTEP views of **5** and **6** are shown in Figures 2 and 3, respectively.

The structure of **2** is rather routine, as the bonding parameters of this complex fall in the expected ranges (details are provided as Supporting Information). In

(7) For a discussion of these aspects concerning Pt(II) complexes, see: Rendina, L. M.; Puddephatt, R. J. *Chem. Rev.* **1997**, *97*, 1735.

(8) (a) Gómez-de la Torre, F.; Jalón, F. A.; López-Agenjo, A.; Manzano, B. R.; Rodríguez, A.; Sturm, T.; Weissensteiner, W.; Martínez-Ripoll, M. *Organometallics* **1998**, *17*, 4634. P,N ancillary ligands have recently been used by Schubert in the preparation of Pt(II) complexes from the corresponding dialkyl derivatives. See: (b) Pfeiffer, J.; Schubert, U. *Organometallics* **1999**, *18*, 3245. See also: (c) Schubert, U.; Kalt, D.; Gilges, H. *Monatsh. Chem.* **1999**, *130*, 207.

Table 1. Experimental Data for the X-ray Diffraction Studies of 2, 5, and 6

	2	5	6
formula	$C_{34}H_{31}Cl_2FeN_2PPd.CH_2Cl_2.CHCl_3$	$C_{34}H_{31}Cl_6FeN_2PPdSi_2.CH_2Cl_2$	$C_{36}H_{35}Cl_6FeN_2PPdSi_2$
fw	936.08	1014.63	957.80
cryst dimens, mm	0.66 × 0.28 × 0.22	0.68 × 0.22 × 0.22	0.8 × 0.56 × 0.08
cryst syst	monoclinic	trigonal	monoclinic
space group (No.)	$P2_1$ (4)	$P3_2$ (145)	$P2_1$ (4)
a (Å)	9.7555(15)	17.966(12)	10.551(2)
b (Å)	20.737(3)	17.966(12)	16.746(3)
c (Å)	10.400(2)	10.785(7)	11.634(2)
α (deg)	90	90	90
β (deg)	107.8370(10)	90	105.28(3)
γ (deg)	90	120	90
V (Å^3)	2002.8(5)	3015(3)	1983.0(5)
Z	2	3	2
ρ(calcd) (g cm^{-3})	1.552	1.676	1.612
μ (mm^{-1})	1.346	1.469	1.354
F(000)	940	1524	974
diffractometer	Siemens SMART PLATFORM with CCD detector		
radiation (λ, Å)	Mo Kα (0.710 73)		
θ range, deg	1.96−28.30	1.31−29.94	1.81−29.72
no. of measd rflns	17 037	22 036	14 545
no. of obsd rflns (n)[a]	7272	10 037	7628
no. of params refined (p)	433	437	440
wR2 ($I > 2\sigma(I)$)[b]	0.1791	0.0950	0.1296
R1 ($I > 2\sigma(I)$)[c]	0.0642	0.0399	0.0535
GOF on F^2 [d]	1.007	1.083	1.007

[a] $|F_o^2| > 4.0\sigma(|F|^2)$. [b] $wR2 = [\sum[w(F_o^2 - F_c^2)^2]/\sum[w(F_o^2)^2]]^{1/2}$. [c] $R1 = \sum||F_o| - |F_c||/\sum|F_o|$. [d] $GOF = S = [\sum[w(F_o^2 - F_c^2)^2]/(n - p)]^{1/2}$.

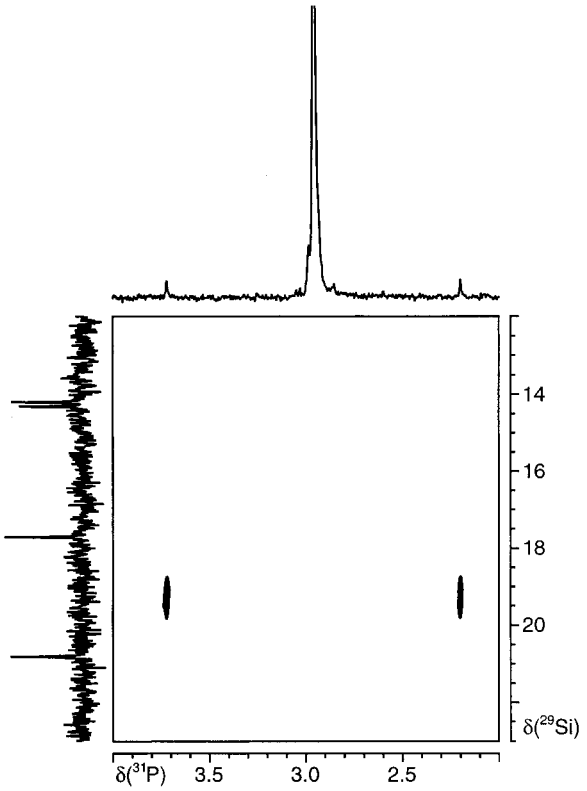

Figure 1. 2D $^{29}Si-^{31}P\{^1H\}$−HMQC spectrum (CD_2Cl_2 solvent, optimized for the large trans coupling constant $^2J(^{31}P,^{29}Si) = 308$ Hz) for complex **5** showing the doublet for the trichlorosilane group trans to the phosphorus spin. Note that the coupling between ^{29}Si and ^{31}P is refocused in the ω_1 (vertical) dimension, while it is not in the conventional 1D spectrum plotted along the left side of the contour area.

particular, bond lengths and angles correspond to those previously observed for similar square-planar complexes containing ferrocenyl phosphino pyrazole ligands.[9] In terms of a comparison with **5** and **6**, the slight twist of 8.7° (N−Pd−P/Cl(1)−Pd−Cl(2) interplanar angle) of the

Table 2. Selected Bond Distances (Å)[a] and Angles (deg)[a] for 2, 5, and 6

	2	5	6
Bond Distances[b]			
Pd−P	2.261(2)	2.4559(16)	2.504(2)
Pd−N(2)	2.083(7)	2.192(4)	2.208(5)
Pd−Si(1) [Pd−Cl(2)]	[2.380(2)]	2.3243(17)	2.309(2)
Pd−Si(2) [Pd−Cl(1)]	[2.259(2)]	2.2594(17)	2.261(2)
Bond Angles[b]			
Si(1)−Pd−P [Cl(2)−Pd−P]	[172.63(6)]	167.78(5)	156.70(8)
Si(2)−Pd−P [Cl(1)−Pd−P]	[94.54(10)]	98.43(7)	100.98(7)
Si(2)−Pd−Si(1) [Cl(1)−Pd−Cl(2)]	[88.98(11)]	87.54(7)	85.81(9)
N(2)−Pd−P	87.1(2)	83.87(11)	91.64(13)
N(2)−Pd−Si(1) [N(2)−Pd−Cl(2)]	[90.0(2)]	92.66(11)	91.2(2)
N(2)−Pd−Si(2) [N(2)−Pd−Cl(1)]	[174.5(2)]	167.20(10)	154.7(2)

[a] Numbers in parentheses are esd's in the least significant digits. [b] Figures in brackets indicate geometrically correspondent bonding parameters for **2**.

square-planar geometry and the Pd−N and Pd−P bond lengths of 2.083(7) and 2.261(2) Å, respectively, are worth noting.

One of the most apparent features of the two bis(trichlorosilyl) complexes is the extreme lengthening of the distances between Pd and the N and P donor atoms. The Pd−P bond lengths of 2.4559(16) (**5**) and 2.504(2) Å (**6**), in particular, are most anomalous. In fact, these are the longest separations in Pd phosphine complexes ever observed.[10] An obvious explanation of this bond elongation is the strong trans influence of the silyl groups.[11,12] On the other hand, the Pd−Si distances fall

(9) Togni, A. In *Metallocenes: Synthesis, Reactivity, Applications*; Togni, A., Halterman, R. L., Eds.; Wiley-VCH: Weinheim, Germany, 1998; pp 685−721 and references therein.

(10) (a) A Pd−P bond length of 2.437(1) Å in a Pd(BINAP)(aryl) complex has recently been claimed to be "world record" and was rationalized on the basis of electronic effects. See: Drago, D.; Pregosin, P. S.; Tschoerner, M.; Albinati, A. *J. Chem. Soc., Dalton Trans.* **1999**, 2279. (b) Magistrato, A.; Merlin, M.; Pregosin, P. S.; Röthlisberger, U.; Albinati, A. Submitted for publication; personal communication.

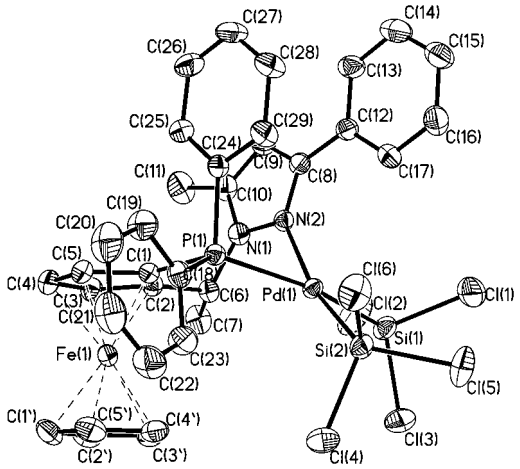

Figure 2. ORTEP plot and atom-numbering scheme of complex **5** (thermal ellipsoids at the 30% probability level).

in the lower range of metal−silicon bond lengths.[1a,13] Moreover, it is important to note that the $SiCl_3$ groups are strongly pyramidalized (average Cl−Si−Cl angles of 102−103° and Pd−Si−Cl angles of 115−116°), with longer Si−Cl distances than in, for example, $HSiCl_3$ or $SiCl_4$.[14] This indicates that the Si−Cl bond has an enhanced p character, resulting in a higher s character for the Pd−Si linkage, according to Bendt's rule,[15] and thus supporting the description of $SiCl_3$ as an excellent π-acceptor.[13,16]

The deviation from the ideal square-planar geometry, as indicated by the angle θ between the P−Pd−N and Si(1)−Pd−Si(2) planes of 17.7° for **5** and 34° for **6** (see also bond angles in Table 2), is another prominent characteristic of these two complexes. In the case of **6**, this tetrahedral distortion is quite severe[17] and could

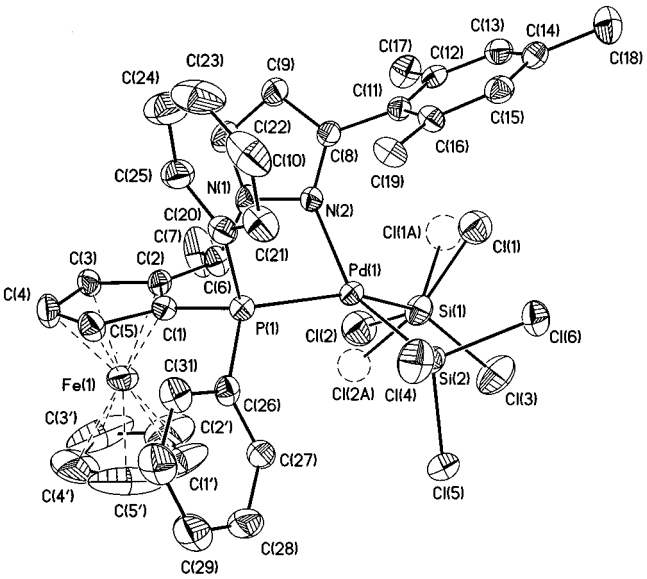

Figure 3. ORTEP plot and atom-numbering scheme of complex **6** (thermal ellipsoids at the 30% probability level). For the two disordered chlorine atoms dashed circles indicate the second equivalent position.

be explained by steric reasons. When inspecting the crystal structure, we attribute the steric congestion in **6** mainly to the presence of the bulky 2,4,6-trimethylphenyl substituent on the pyrazole. This fragment is assuming an almost orthogonal orientation with respect to the pyrazole ring and "pushes away" the $SiCl_3$ group trans to phosphorus. It also appears to be responsible for the distorted orientation of the pyrazole with respect to Pd. In fact, the N(2)−Pd vector forms an angle φ of 18.2° with the least-squares plane of the heterocycle, the ideal expected value being $\varphi = 0°$ (for **5** this angle is 4.7°). It is therefore conceivable that the Pd−N bond is significantly weakened because of a nonideal orbital overlap, thus having important implications for catalytic hydrosilylations using the corresponding ligand, as it was postulated that Pd−N bond breaking might be a necessary step in the catalytic cycle.[6]

In view of the magnitude of the geometric distortions found in complex **6** and with the aim of ascertaining their exact origin, we have performed a computational investigation of these derivatives in the framework of a combined quantum mechanics and molecular mechanics method.

QM/MM Study: General Considerations. To examine the nature of the unusual geometric distortions observed in the X-ray structures of complexes **5** and **6**, we have performed a series of density functional theory (DFT) and combined quantum mechanics and molecular mechanics (QM/MM) calculations.[18] Although the com-

(11) (a) Brost, R. D.; Bruce, G. C.; Joslin, F. L.; Stobart, S. R. *Organometallics* **1997**, *16*, 5669. (b) Hofmann, P.; Meier, C.; Hiller, W.; Heckel, M.; Riede, J.; Schmidt, M. U. *J. Organomet. Chem.* **1995**, *490*, 51. (c) Levy, C. C.; Puddephatt, R. J.; Vittal, J. J. *Organometallics* **1994**, *13*, 1559. (d) Pham, E.; West, R. *Organometallics* **1990**, *9*, 1517. (e) Sakaki, S.; Ogawa, M.; Musashi, Y.; Arai, T. *J. Am. Chem. Soc.* **1994**, *116*, 7258. (f) Sakaki, S.; Ujino, Y.; Sugimoto, M. *Bull. Chem. Soc. Jpn.* **1996**, *69*, 3047. (g) Yamashita, H.; Hayashi, T.; Kobayashi, T.; Tanaka, M.; Goto, M. *J. Am. Chem. Soc.* **1988**, *110*, 4417.

(12) Silyl ligands also display a large kinetic trans effect. See: Wendt, O. F.; Elding, L. I. *Inorg. Chem.* **1997**, *36*, 6028.

(13) The shorter M−Si bond lengths for electron-rich late transition metals have been attributed to M→Si π-back-bonding. See, e.g.: (a) Hübler, K.; Hunt, P.; Maddock, S. M.; Rickard, C. E. F.; Roper, W. R.; Salter, D. M.; Schwerdtfeger, P.; Wright, L. J. *Organometallics* **1997**, *16*, 5076. (b) Koga, N.; Morokuma, K. *J. Am. Chem. Soc.* **1993**, *115*, 6883. (c) Koloski, T. S.; Pestana, D. C.; Carroll, P. J.; Berry, D. H. *Organometallics* **1994**, *13*, 489. (d) Lichtenberger, D. L.; Rai-Chaudhuri, A. *Inorg. Chem.* **1990**, *29*, 975. (e) Orpen, A. G.; Connelly, N. G. *Organometallics* **1990**, *9*, 1206. (f) Orpen, A. G. *Chem. Soc. Rev.* **1993**, 191. (g) Dunne, B. J.; Morris, R. B.; Orpen, A. G. *J. Chem. Soc., Dalton Trans.* **1991**, 653. It has also been pointed out that the more electronegative late transition-metals are able to polarize the M−Si bond, thus enhancing the electrostatic bond component shortening the bond. See: (g) Jiang, Q.; Pestana, D. C.; Carroll, P. J.; Berry, D. H. *Organometallics* **1994**, *13*, 3679.

(14) Sheldrick, W. S. *Structural Chemistry of Organic Silicon Compounds*; Patai, S., Rappoport, Z., Eds.; Wiley: New York, 1989; pp 228−294.

(15) Bent, H. A. *Chem. Rev.* **1961**, *61*, 275.

(16) See, e.g.: (a) Jagirdar, B. R.; Palmer, R.; Klabunde, K. J.; Radonovic, L. J. *Inorg. Chem.* **1995**, *34*, 278. (b) Robinson, W. T.; Ibers, J. A. *Inorg. Chem.* **1967**, *6*, 1208. (c) Yao, Z.; Klabunde, K. J.; Asirvatham, A. S. *Inorg. Chem.* **1995**, *34*, 5289. (d) Glavee, G. N.; Jagirdar, B. R.; Schneider, J. J.; Klabunde, K. J.; Radonovic, L. J.; Dodd, K. *Organometallics* **1992**, *11*, 1043. A Ni complex showing an opposite trend (longer Si−Cl bonds and larger Cl−Si−Cl angles) has been reported: Janikowski, S. K.; Radonovich, L. J.; Groeshens, T. J.; Klabunde, K. J. *Organometallics* **1985**, *4*, 396.

(17) A similar twist of 38° has been reported recently for the Pt complex *cis*-$[Pt(SiPh_2Me)_2(PMe_2Ph)_2]$. See: Tsuji, Y.; Nishiyama, K.; Hori, S.; Ebihara, M.; Kawamura, T. *Organometallics* **1998**, *17*, 507. For a recent example of a rare Pd(II) high-spin tetrahedral complex, having a $PdCl_2O_2$ coordination sphere, see: Yeo, J. S. L.; Vittal, J. J.; Hor, T. S. A. *J. Chem. Soc., Chem. Commun.* **1999**, 1477.

(18) (a) Gao, J.; Thompson, M. *Methods and Applications of Combined Quantum Mechanical and Molecular Mechanical Methods*; American Chemical Society: Washington, DC, 1998. (b) Singh, U. C.; Kollman, P. A. *J. Comput. Chem.* **1986**, *7*, 718−730. (c) Field, M. J.; Bash, P. A.; Karplus, M. *J. Comput. Chem.* **1990**, *11*, 700−733. (d) Gao, J. Review on QM/MM. In *Reviews in Computational Chemistry*; Lipkowitz, K. B., Boyd, D. B., Ed.; VCH: New York, 1996; Vol. 7, pp 119−185.

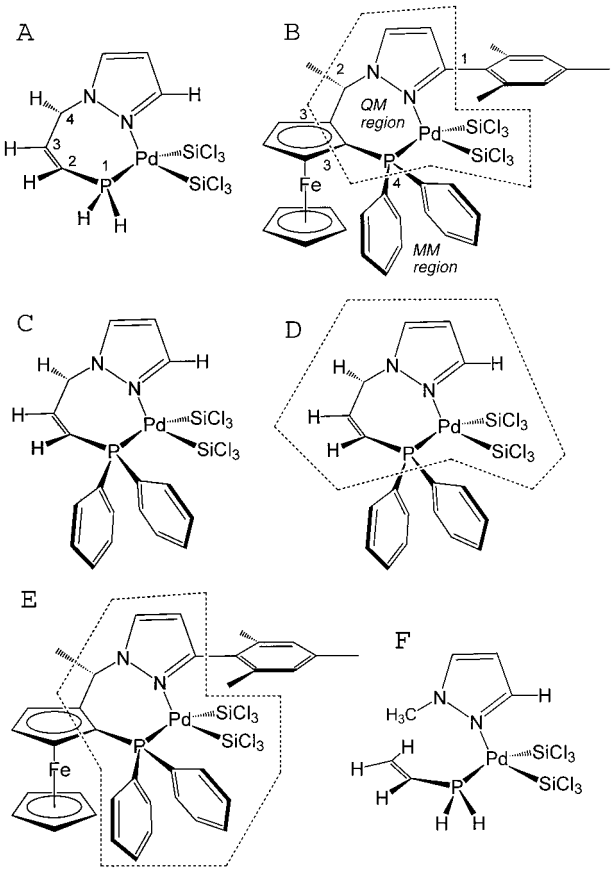

Figure 4. Structural representation of computational models **A**−**F**. Models **B**, **D**, and **E** are combined QM/MM models where the regions enclosed in the dotted polygons represent the QM region. The regions outside the polygons are treated by a molecular mechanics force field. For the electronic structure calculation of the QM region, the covalent bonds that traverse the QM/MM boundary (the dotted polygon) have been capped with hydrogen atoms. In model **A** the atoms labeled 1−4 are the atoms that have been fixed in the calculations of models **A**−**E**.

putational resources to wholly treat both **5** and **6** at the DFT level are available, we have employed the combined QM/MM method to disentangle the steric factors from the electronic effects that influence the distortions observed. With the combined QM/MM method, part of the molecular system is treated with an electronic structure calculation, in this case DFT, while the remainder of the complex is treated with a molecular mechanics approach. The different models **A**−**F** that have been examined in this study are illustrated in Figure 4, also indicating the QM/MM partitioning for models **B**, **D**, and **E**.

There exist many varieties of QM/MM methods. In the IMOMM[19] approach that we have utilitized, electronic effects across covalent bonds that traverse the QM/MM boundary are for the most part neglected. The primary reason for this is that the electronic structure calculation is performed on a truncated "QM model system", whereby the boundary bonds are terminated with "capping" atoms, usually hydrogens. The capping atoms satisfy the valence requirements across the boundary bonds such that a standard electronic structure calculation can be performed on the QM model system. The important point is that, with the QM/MM approach that has been utilized, only the steric influences of the fragments contained in the MM region are modeled. For example, in the QM/MM model **B**, only the steric influence, not the electronic donor/acceptor properties, of the phosphine phenyl groups is accounted for (more precisely, the electronic effects of the phenyl rings are made equivalent to those of the capping atoms). Although this is often a serious limitation with the QM/MM method, it can be taken as an advantage in view of separating as much as possible the steric and electronic effects of specific molecular fragments. Finally, note that in the models **A**, **C**, **D**, and **F** the ferrocenyl moiety has been replaced with an olefinic group in order to reduce the computational expense of the calculations. However, the C−C bond distance in the cyclopentadienyl ring of 1.44 Å is significantly larger than that of a typical olefin (∼1.33 Å). Thus, to preserve the structural features imposed by the ferrocenyl group on the chelating backbone, constraints have been applied. For the complete QM/MM models of complexes **5** and **6**, only this C−C bond distance was constrained, whereas for the partial models the entire P−C(Cp)−C(Cp)−C−N(1) backbone was fixed (see the Supporting Information for full computational details).

(19) Maseras, F.; Morokuma, K. *J. Comput. Chem.* **1995**, *16*, 1170.

Table 3. Comparison of Selected Geometric Parameters Derived from the Experimental X-ray Structure of 6 and Those of the Various Calculated Models

			model					
param[a]	exptl X-ray	full QM[b]	**A**[c]	**B**[c]	**C**[c]	**D**[c]	**E**[c]	**F**[c]
Pd−P	2.50	2.53	2.39	2.46	2.42	2.40	2.50	2.39
Pd−N	2.21	2.25	2.18	2.20	2.19	2.19	2.21	2.19
Pd−Si(1)	2.31	2.33	2.33	2.32	2.34	2.34	2.32	2.35
Pd−Si(2)	2.26	2.29	2.29	2.28	2.29	2.30	2.28	2.30
P−Pd−N/Si−Pd−Si plane angle	34.0	35.7	11.8	30.4	18.6	15.8	34.6	1.4
pyrazole plane/N−Pd angle	18.2	14.9	4.0	15.7	2.1	3.9	12.5	2.1
pyrazole/phenyl plane angle[d]	65.4	68.6		63.2			62.7	-

[a] Distances reported in Å and angles reported in deg. [b] This refers to the fully optimized structure of **6** that was wholly calculated at the DFT level. [c] See Figure 4 and text for description of model systems **A**−**D**. [d] This refers to the angle between the ring planes of the pyrazole ring and the phenyl substituent to which it is bound.

Accuracy of the DFT Approach. The accuracy of the quantum-mechanical method chosen can be assessed by comparing the experimental solid-state X-ray structure of complex **6** with that of the optimized (gas-phase) structure, where the whole complex has been calculated at the DFT level. Without imposition of any geometric constraints, the agreement is excellent, as illustrated by the second and third columns of Table 3, in which key geometric parameters of the experimental and calculated structures are compared. Both the extraordinarily long Pd−P distance and the non-square-planar geometry at the metal center are reproduced remarkably well. Specifically, the calculated Pd−P distance is within 0.03 Å of the X-ray structure and the angle θ between the planes defined by the N−Pd−P and the Pd−Si−Si triads is within 2° of the experimental value. The most notable deviation is in the Pd−N bond distance, which is calculated to be 2.25 Å, or 0.04 Å longer than that found in the X-ray structure.

Nature of the Pd−P Elongation. The nature of the extreme lengthening of the Pd−P bonds in the two bis(trichlorosilyl) complexes **5** and **6** has been examined with a particular emphasis on separating the steric from the electronic influences. Although an obvious rationalization for the anomalous Pd−P distances is the strong trans influence of the silyl group (vide supra), another plausible explanation involves the steric pressure that is exerted on the Pd−P bond due to the interaction of the phenyl groups with the bulky trichlorosilyl fragments. To pinpoint the nature of the elongation, we have generated a systematic series of model systems, in which the steric and electronic influences of the phenyl ligands have been selectively altered. We start with the QM model **A**.

Key geometric parameters for the optimized structure of model **A** are detailed in the fourth column of Table 3. The removal of the phenyl substituents of the phosphine and the trimethylphenyl substituent of the pyrazole ring results in a significant contraction of the Pd−P bond from 2.504 to 2.39 Å. We note that a distance of 2.39 Å for a Pd−P bond still lies in the upper end of the literature range, with a distance of 2.437 Å being recently reported.[10] From model **A** it can be concluded that both sets of phenyl substituents in **5** and **6** are principal components in the extreme lengthening of the Pd−P bond. Thus, the "world record" lengthening cannot be fully explained in terms of the trans influence of the silyl groups.

Next let us examine a QM/MM model system of complex **6** where the steric influence of the phenyl substituents and of the ferrocene is accounted for but the electronic effects have been largely eliminated (model **B**). In other words, the peripheral groups have been delegated to the MM region, while the molecular system used for electronic structure calculation has been kept identical with that in model **A**.

Table 3 reveals that, in comparison to model **A**, the Pd−P bond distance in model B is elongated from 2.39 to 2.46 Å. Thus, it can be concluded that the steric influence of the phenyl substituents plays a substantial role in the elongation of the Pd−P bond in **6**. Note that the trimethylphenyl substituent of the pyrazole ring in **6** is oriented perpendicular to its host. This results in a strong steric interaction between the trimethylphenyl group and one of the phenyls of the phosphine, thus putting pressure on the Pd−P bond. Although the results of these two model systems suggest that the steric influence of the phenyl substituents is a significant factor in the long Pd−P bond distance observed in **6**, they do not account for it completely. For example, the Pd−P bond distance of 2.46 Å in **5** is also extremely long, even though the phenyl substituent of the pyrazole ring in **5** lies almost coplanar to its host. Perhaps part of the lengthening observed in model **B**, as compared to model **A**, is a result of the interaction between the phosphine phenyl rings and one of the bulky trichlorosilyl groups (see also model **C** below).

With the next model, we attempt to isolate the effect of the phosphine phenyl substituents from that of the trimethylphenyl group on the pyrazole ring. Thus, in the pure QM model **C** the electronic structure of the phenyl rings of the phosphine is treated explicitly, but the trimethylphenyl group is completely removed (replaced by hydrogen). Table 3 shows that, in comparison to model **A**, explicit treatment of the phosphine phenyl groups results in a moderate elongation of the Pd−P distance from 2.39 to 2.42 Å. This lengthening of the Pd−P bond in model **C** could be attributed to the electronic and/or steric influence of the PPh_2 group compared to the PH_2 in model **A**.

To separate the steric effects of the phenylphosphine groups from their electronic effect, model **D** was constructed. This model is similar to model **C** except that the phenyl rings are treated by a molecular mechanics potential. Thus, with model **D**, only the steric influence of the phenylphosphines is modeled. The Pd−P distance in model **D** is 2.40 Å, revealing that the steric lengthening of the Pd−P bond due to the interaction between the $SiCl_3$ fragments and the phosphine phenyl groups is minimal. Thus, it can be concluded that, in comparison to PH_2, the PPh_2 group plays a role in elongating the Pd−P bond through electronic effects, as one would qualitatively expect on the basis of the donor ability of these two fragments. An examination of the Mulliken charges on the P atom in model **A** compared to **C** is consistent with this picture. In model **A** the phosphorus has a calculated Mulliken charge of +0.12 e, whereas it is determined more electron deficient in model **C** with a Mulliken charge of +0.25 e.

Comparison of the Pd−P bond distance in model **B** with that of model **D** suggests that much of the lengthening of the Pd−P bond in complex **6** results from the steric interaction between the phenyl groups of the phosphine and the trimethylphenyl group of the pyrazole ring. As discussed above, this interaction is strong in complex **6** due to the orientation of the trimethylphenyl group. The primary difference between models **B** and **D** is that in the latter the steric interaction between the two substituent groups is absent. Therefore, it can be concluded that this steric interaction approximately accounts for an elongation of the Pd−P bond from 2.40 Å (model **D**) to 2.46 Å (model **B**). Additionally, there is a minimal elongation due to the interaction between the phosphine phenyl groups and one of the bulky trichlorosilyl groups.

The results of the various model systems corroborate the implication that the steric interaction between the phosphine phenyls and the trimethylphenyl group significantly weakens the Pd−N bond in complex **6**. This was discussed in terms of the observed distortion of the pyrazole ligand with respect to the Pd center. In models **A**, **C**, and **D**, this distortion is absent because of the removal of the trimethylphenyl group, as indicated by the small angles φ (vide supra) of 4.0, 2.1, and 3.9°, respectively. On the other hand, the experimental angle φ for **6** of 18° is well-reproduced in the full QM structure of **6** (15°) and in model **B** (16°).

Finally, we have constructed QM/MM models of complexes **5** and **6**, whereby the phenylphosphine groups are contained in the QM region, while the ferrocenyl and phenyl substituents on the pyrazoles are accounted for on a steric basis only (model **E** for **6** and **G** for **5**, the latter not depicted in Figure 4). The agreement between the X-ray structure of **6** and model **E** is remarkable. For example, both the Pd−P distance and the twist of the coordination plane of the Pd center are virtually identical with those of the X-ray structure.

Table 4. Comparison of Selected Geometric Parameters Derived from the Experimental X-ray Structure of 5 with That of the Calculated QM/MM Model

param[a]	exptl X-ray	model **G**
Pd−P	2.46	2.47
Pd−N	2.19	2.21
Pd−Si(1)	2.32	2.34
Pd−Si(2)	2.26	2.29
P−Pd−N(2)/Si−Pd−Si plane angle	17.7	17.2
pyrazole plane/N(2)−Pd angle	4.7	2.6
pyrazole/phenyl plane angle	11.7	11.4

[a] Distances reported in Å and angles reported in deg.

In fact, the selected parameters displayed in Table 3 are generally better than those of the full QM calculation.

The agreement between the X-ray structure of **5** and model **G** is equally impressive, as evidenced by the comparison provided in Table 4. The Pd−P bond distance in model **G** is calculated to be 2.47 Å, close to the experimental value of 2.46 Å, suggesting that there is still a strong steric interaction between the phenyl ring of the pyrazole and the phosphine phenyl groups, despite the different conformation as compared to **6**.

Nature of the Non-Square-Planar Coordination of the Pd Center. Both complexes **5** and **6** possess an anomalous non-square-planar coordination geometry of the Pd center, as indicated by the angle θ between the planes defined by the P−Pd−N(2) and Pd−Si−Si atoms, as defined above. Model **A** has a slightly distorted square planar geometry, as demonstrated by the θ angle of 11.8° (Table 3). This is somewhat surprising, since the pendant phenyl groups on the pyrazole ring and the phosphine are not present in this model. Thus, even without the presence of these groups there is a slight preference away from the ideal square-planar geometry. Detailed examination of the geometry reveals that the structure of the Pd−ferrocenyl−phosphine−pyrazole chelate ring orients the pyrazole such that there is a notable steric interaction between the substituent in the 3-position (in this case H) of the heterocycle with the trichlorosilyl group trans to the phosphine.[20] Figure 5 depicts this interaction for model **A** if an ideal square planar coordination is enforced.

In model **F**, the chelate ring is broken, thereby removing the imposed orientation on the pyrazole fragment. Optimization of model **F** reveals that a near-ideal square-planar structure is favored with a θ angle of 1.4°. Interestingly, when the optimization of model **F** is initiated from a distorted structure, a non-square-planar stationary point with an θ angle of 25° is located 4.5 kcal/mol above that of the planar structure. Thus, it can be concluded that despite the electronic preference for the square-planar coordination of the Pd center, the steric effects imposed by the structure of the chelate ring result in a slight distortion of the structure.

In the X-ray structures of both **5** and **6**, the tetrahedral distortion is greater than that found in model **A**. Since there is an electronic preference for a square-planar coordination, the pendant phenyl substituents in **5** and **6** likely result in further steric crowding and therefore in more distorted structures compared to model **A**. In the QM/MM model **B** an optimized θ angle of 30° is found, close to the 34° angle of the X-ray structure. Since the phenyl and trimethylphenyl groups are accounted for on a steric basis only in model **B**, the result supports the notion that the severely distorted coordination of the Pd center in **6** is due to a steric effect.

(20) Several orientations of the trichlorosilyl ligands were optimized, starting from both bent and square-planar structures. All optimizations lead to complexes with slightly distorted square planar geometries.

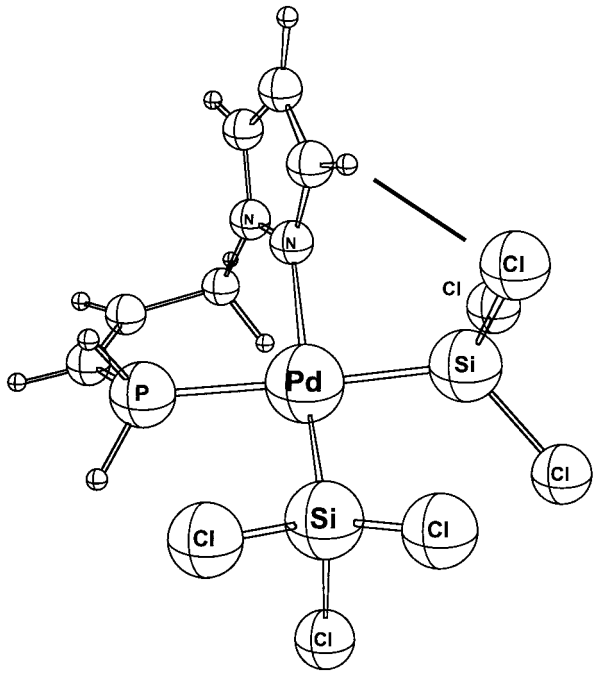

Figure 5. Geometry of model **A** showing the steric interaction between the trichlorosilyl ligand and the hydrogen at the 3-position of the pyrazole ring that results in a slight deviation from the intrinsic square-planar coordination geometry at Pd.

In models **C** and **D** the phenyl substituent of the pyrazole ring is not present, and here the θ angles are 19 and 16°, respectively. Even without the trimethylphenyl moiety, the Pd coordination is more distorted than in model **A**, suggesting that the phenyl rings of the phosphine enhance the distortion. Furthermore, since the magnitude of the distortion observed in model **C** is almost the same as that in model **D**, it can be concluded that the effect of the phenylphosphine groups on the coordination geometry is steric in nature and not electronic.

Model **G**, the QM/MM model of complex **5**, has a θ angle of only 17°, which is approximately the same as that in models **C** and **D**. This indicates that, beyond the distortion observed in model **A**, the phenyl substituent of the pyrazole ring does not contribute significantly to the distortion at the Pd center. This is also evidenced by the fact that this phenyl ring is twisted with respect to the pyrazole ring toward the proximate trichlorosilyl group.

Conclusions

We have shown that Pd dichloro complexes of types **1**−**3** smoothly react with an excess of trichlorosilane, affording in good yields the corresponding bis(trichlorosilyl) derivatives. Instead of using the QM/MM approach to simply handle the large size of the compounds studied, the method has been effectively used as an analytical tool to probe the nature of the unique

structures observed in complexes **5** and **6**, in particular by separating the steric from the electronic factors.[30] Thus, the extreme lengthening of the Pd−P bonds in **5** and **6** is a combination of electronic and steric effects. In this respect, the phosphine phenyl substituents contribute to the Pd−P bond lengthening on both a steric and an electronic level. The strong trans influence of the trichlorosilyl ligand is enhanced by the presence of the phosphine phenyl groups. In **6**, the "world record" Pd−P bond distance can be primarily attributed to the strong steric interaction between the PPh_2 group with the trimethylphenyl fragment on the pyrazole ring.

The deviation from the square-planar geometry at the Pd center in complexes **5** and **6** can be attributed wholly to steric factors. Calculations have shown that there is a moderate electronic preference favoring the planar coordination, amounting to approximately 4.5 kcal/mol. However, steric interactions between the bulky trichlorosilyl ligands with both phenyl substituents of the phosphine and pyrazole ring result in a distortion away from the ideal square-planar geometry. We further have found that the framework of the specific chelate backbone positions the pyrazole ring such that these interactions are enhanced. We are currently performing further combined experimental/theoretical studies addressing mechanistic aspects of the asymmetric hydrosilylation reaction catalyzed by complexes of type **1**−**3**. We shall be reporting on this in due course.

Computational Details

The density functional theory calculations were performed with the ab initio molecular dynamics package CPMD.[21] The gradient-corrected exchange functional of Becke[22] and the correlation functional of Perdew[23,24] were utilized in conjunction with the LDA parametrization of Goedecker et al.[25] The valence orbitals were expanded in the basis of plane waves with a kinetic energy cutoff of 70 Ry. For the combined QM/MM calculations the CPMD package was modified[26] according to the IMOMM method of Maseras and Morokuma.[19,27] The Tripos 5.2 force field[28] was utilized for the molecular mechanics potential. To accommodate the ferrocenyl ligand, the Tripos force field was augmented according to the ferrocene force field developed by Doman et al.[29] For each of the model complexes **A**−**G**, the geometry optimization was initiated from several conformations, including an ideal square-planar conformation and a conformation taken from the equivalent X-ray structure. The geometries given in Tables 3 and 4 represent the lowest energy conformations found. Full details of the computations are provided as Supporting Information.

(21) Hutter, J.; Ballone, P.; Bernasconi, M.; Focher, P.; Fois, E.; Goedecker, S.; Parrinello, M.; Tuckerman, M. CPMD; Max-Planck-Institut für Festkörperforschung, Stuttgart, Germany, and IBM Zürich Research Laboratory, 1998.
(22) Becke, A. *Phys. Rev. A* **1988**, *38*, 3098.
(23) Perdew, J. P. *Phys. Rev. B* **1986**, *34*, 7406.
(24) Perdew, J. P. *Phys. Rev. B* **1986**, *33*, 8822.
(25) Goedecker, S.; Hutter, J.; Teter, M. *Phys. Rev. B* **1996**, *54*, 1703.
(26) Woo, T. K.; Röthlisberger, U. Unpublished work.
(27) Woo, T. K.; Cavallo, L.; Ziegler, T. *Theor. Chem. Acta* **1998**, *100*, 307.
(28) Clark, M.; Cramer, R. D., III; Van Opdenbosch, N. *J. Comput. Chem.* **1989**, *10*, 982.
(29) Doman, T. N.; Landis, C. R.; Bosnich, B. *J. Am. Chem. Soc.* **1992**, *114*, 7264.
(30) For other reports concerning this aspect, see, e.g.: (a) Deng, L.; Woo, T. K.; Cavallo, L.; Margl, P. M.; Ziegler, T. *J. Am. Chem. Soc.* **1997**, *119*, 6177. (b) Cavallo, L.; Woo, T. K.; Ziegler, T. *Can. J. Chem.* **1998**, *76*, 1457. (c) Woo, T. K.; Ziegler, T. *J. Organomet. Chem.*, in press. (d) Ujaque, G.; Maseras, F.; Lledós, A. *J. Am. Chem. Soc.* **1999**, *121*, 1317.

Experimental Section

Dichloro{1-{(*R*)-1-[(*S*)-2-(diphenylphosphino-κ*P*)ferrocenyl]ethyl}-3,5-dimethyl-1*H*-pyrazole-κ*N*}palladium (1). [Pd(COD)Cl_2] (110 mg, 0.386 mmol) and 1-{(*R*)-1-[(*S*)-2-(diphenylphosphino)ferrocenyl]ethyl}-3,5-dimethyl-1*H*-pyrazole (200 mg, 0.406 mmol) were stirred for 15 min in CH_2Cl_2 (4 mL). Et_2O (5 mL) was added, and the product precipitated. The red solid was filtered off, washed twice with Et_2O (5 mL), and dried in vacuo. Yield: 214 mg, 81%. Mp: >222 °C dec. ^{1}H NMR (250.131 MHz, $CDCl_3$): δ 7.90−7.82 (m, 2 H, Ph *H*), 7.61 (q, 1 H, C*H*MeN, *J* = 7 Hz), 7.51−7.30 (m, 4 H, Ph *H*), 7.24−7.17 (m, 2 H, Ph *H*), 6.94−6.86 (m, 2 H, Ph *H*), 5.38 (s, 1 H, Py *H*), 4.84 (m, 1 H, C_5H_3), 4.47 (m, 1 H, C_5H_3), 4.33 (s, 5 H, C_5H_5), 3.67 (m, 1 H, C_5H_3), 2.20 (s, 3 H, Py *Me*), 2.11 (d, 3 H, CH*Me*N, *J* = 7), 1.88 (s, 3 H, Py *Me*). ^{13}C{^{1}H} NMR (62.903 MHz, $CDCl_3$): δ 150.48−126.1 (Ph *C*, Py *C*), 110.7 (Py *C*H), 90.8 (d, C_5H_3, *J* = 15 Hz), 74.5 (C_5H_3), 71.5 (C_5H_5), 70.9 (d, C_5H_3, *J* = 7), 70.1 (d, C_5H_3, *J* = 56), 68.9 (d, C_5H_3, *J* = 7), 16.7, 14.1, 12.8 (Py *Me*, CH*Me*N). ^{31}P{^{1}H} NMR (101.259 MHz, $CDCl_3$): δ 6.2 (*P*Ph_2). MS (FAB$^+$): *m*/*z* 670 ([M]$^+$, 11%), 633 ([M − Cl]$^+$, 100%). Anal. Calcd for $C_{29}H_{29}Cl_2FeN_2PPd\cdot{}^1/_4CH_2Cl_2$: C, 50.84; H, 4.30; N, 4.05. Found: C, 51.04, H, 4.17, N, 4.10.

Dichloro{1-{(*R*)-1-[(*S*)-2-(diphenylphosphino-κ*P*)ferrocenyl]ethyl}-3-phenyl-5-methyl-1*H*-pyrazole-κ*N*}-palladium (2). This compound was obtained from [Pd(COD)Cl_2] (78 mg, 0.274 mmol) and 1-{(*R*)-1-[(*S*)-2-(diphenylphosphino)ferrocenyl]ethyl}-3-phenyl-5-methyl-1*H*-pyrazole (160 mg, 0.289 mmol), analogously to **1**. Yield: 167 mg, 83%. Mp: >235 °C dec. ^{1}H NMR (300 MHz, CD_2Cl_2): δ 8.41 (q, 1 H, C*H*MeN, *J* = 7 Hz), 8.23 (m, 2 H, Ph *H*), 7.82−7.77 (m, 2 H, Ph *H*), 7.55−7.49 (m, 1 H, Ph *H*); 7.42−7.34 (m, 5 H, Ph *H*), 7.23−7.16 (m, 1 H, Ph *H*), 6.89−6.83 (m, 2 H, Ph *H*), 6.59−6.51 (m, 2 H, Ph *H*), 5.91 (s, 1 H, Py *H*), 4.99 (m, 1 H, C_5H_3), 4.57 (m, 1 H, C_5H_3), 4.50 (s, 5 H, C_5H_5), 3.71 (m, 1 H, C_5H_3), 2.31 (s, 3 H, Py *Me*), 2.24 (d, 3 H, CH*Me*N, *J* = 7). ^{13}C{^{1}H} NMR (62.89 MHz, CD_2Cl_2): δ 151.9−126.3 (Ph *C*, Py *C*), 109.8 (Py *C*), 90.4 (d, C_5H_3, *J* = 15 Hz), 74.8 (C_5H_3), 71.8 (C_5H_5), 70.8 (d, C_5H_3, *J* = 7), 70.5 (d, C_5H_3, *J* = 57), 69.3 (d, C_5H_3, *J* = 7), 60.9 (C*H*MeN), 16.7 (CH*Me*N), 13.2 (Py *Me*). ^{31}P{^{1}H} NMR (121.50 MHz, CD_2Cl_2): δ 8.59. MS (FAB$^+$): *m*/*z* 730 ([M]$^+$, 7%), 695 ([M − Cl]$^+$, 100%). Anal. Calcd for $C_{34}H_{31}Cl_2FeN_2PPd$: C, 55.81; H, 4.27; N, 3.83. Found: C, 55.93, H, 4.37, N, 3.68. Crystals suitable for X-ray diffraction were grown from mixtures of CH_2Cl_2 and $CHCl_3$.

Dichloro{1-{(*R*)-1-[(*S*)-2-(diphenylphosphino-κ*P*)ferrocenyl]ethyl}-3-(2,4,6-trimethylphenyl)-1*H*-pyrazole-κ*N*}-palladium (3). This compound was obtained from [Pd(COD)Cl_2] (82 mg, 0.286 mmol) and 1-{(*R*)-1-[(*S*)-2-(diphenylphosphino)ferrocenyl]ethyl}-3-(2,4,6-trimethylphenyl)-1*H*-pyrazole (160 mg, 0.289 mmol), analogously to **1**. Yield: 162 mg, 75%. Mp: >186 °C dec. ^{1}H NMR (250 MHz, CD_2Cl_2): δ 8.11−7.93 (m, 4 H, Ph *H*), 7.81 (d, 1 H, Py *H*, *J* = 3 Hz), 7.75−7.65 (m, 1 H, Ph *H*), 7.62−7.48 (m, 5 H, Ph *H*), 7.05−6.82 (m, 2 H, Mes *H*, C*H*MeN), 6.78 (s, 1 H, Mes *H*), 6.21 (d, 1 H, Py *H*, *J* = 3), 4.42 (m, 1 H, C_5H_3), 4.33 (m, 1 H, C_5H_3), 4.29 (m, 1 H, C_5H_3), 3.90 (s, 5 H, C_5H_5), 2.37 (s, 3 H, Mes *Me*), 2.33 (d, 3 H, CH*Me*N, *J* = 7), 2.25 (s, 3 H, Mes *Me*), 1.09 (s, 3 H, Mes *Me*). ^{13}C{^{1}H} NMR (CD_2Cl_2): δ 156.4−125.5 (Ph *C*, Mes *C*, Py *C*), 110.8 (Py *C*), 91.7 (d, C_5H_3, *J* = 21 Hz), 74.4 (d, C_5H_3, *J* = 3), 73.4 (d, C_5H_3, *J* = 55), 70.9 (C_5H_5), 69.8 (d, C_5H_3, *J* = 7), 66.2 (d, C_5H_3, *J* = 7), 57.9 (*C*HMeN), 21.6 (Mes *Me*), 21.0 (Mes *Me*), 20.7 (Mes *Me*), 17.1 (CH*Me*N). ^{31}P{^{1}H} NMR (101.26 MHz, CD_2Cl_2): δ 11.2. MS (FAB$^+$): *m*/*z* 723 ([M − Cl]$^+$, 98%). Anal. Calcd for $C_{36}H_{35}Cl_2FeN_2PPd$: C, 56.91; H, 4.64; N, 3.69. Found: C, 56.63, H, 4.69, N, 3.52.

Bis(trichlorosilyl)-{1-{(*R*)-1-[(*S*)-2-(diphenylphosphino-κ*P*)ferrocenyl]ethyl}-3,5-dimethyl-1*H*-pyrazole-κ*N*}-palladium (4). To a solution of **1** (200 mg, 0.298 mmol) in CH_2Cl_2 (4 mL) was added $HSiCl_3$ (1 mL, 5.5 mmol), and the mixture was stirred for 3 days. The solution turned from red

to yellow. The product was precipitated by adding hexane (10 mL) and was filtered off, washed twice with hexane (10 mL), and dried in vacuo, affording an air- and moisture-sensitive powder. Yield: 196 mg, 76%. ^{1}H NMR (250 MHz, $CDCl_3$): δ 7.7−7.36 (m, 5 H, Ar *H*), 7.33−7.22 (m, 1 H, Ar *H*), 7.20−7.08 (m, 2 H, Ar *H*), 6.83−6.69 (m, 2 H, Ar *H*), 6.38 (q, 1 H, C*H*MeN, J = 7 Hz), 5.34 (s, 1 H, Py *H*), 4.81 (m, 1 H, C_5H_3), 4.47 (m, 1 H, C_5H_3), 4.32 (m, 1 H, C_5H_5), 3.52 (m, 1 H, C_5H_3), 2.18 (s, 3 H, Py *Me*), 2.03 (d, 3 H, CH*Me*N, J = 7), 1.75 (s, 3 H, Py *Me*). ^{13}C{^{1}H} NMR ($CDCl_3$): δ 148.4−127.7 (Ar *C*, Py *C*), 109.6 (Py *C*), 89.8 (d, C_5H_3, J = 16 Hz), 75.5 (C_5H_3), 73.7 (d, C_5H_3, J = 36), 71.2 (C_5H_5), 70.6 (d, C_5H_3, J = 5), 69.2 (d, C_5H_3, J = 6), 16.9, 13.9, 12.3 (CH*Me*N, Py *Me*). ^{31}P{^{1}H} NMR (101.26 MHz, $CDCl_3$): δ 6.9 (PPh_2, J(P,Si_{trans}) = 317). ^{29}Si NMR (99.4 MHz, $CDCl_3$): δ 20.4 (Si trans tro P, ^2J(Si_{trans},P) = 317), 16.4 (Si trans to N). Anal. Calcd for $C_{29}H_{29}N_2PFePdSi_2Cl_6$: C, 40.14; H, 3.37; N, 3.23. Found: C, 40.92; H, 3.82; N, 2.99.

Bis(trichlorosilyl)-{1-{(*R*)-1-[(*S*)-2-(diphenylphosphino-κ*P*)ferrocenyl]ethyl}-3-phenyl-5-methyl-1*H*-pyrazole-κ*N*}-palladium (5). This compound was obtained from **2** (150 mg, 0.205 mmol) in CH_2Cl_2 (4 mL) and $HSiCl_3$ (1 mL, 5.5 mmol) by following the procedure described for **4**. Yield: 160 mg, 84%. Crystals suited for X-ray diffractometry were obtained by slow diffusion of pentane into a solution of **5** in CH_2Cl_2. ^{1}H NMR (250 MHz, $CDCl_3$): δ 7.92−7.6 (m, 3 H, Ar *H*), 7.58−7.1 (m, 7 H, Ar *H*), 7.08−6.95 (q, 1 H, C*H*MeN, J = 7 Hz), 6.92−6.76 (m, 2 H, Ar *H*), 6.75−6.5 (m, 3 H, Ar *H*), 5.93 (s, 1 H, Py *H*), 4.85 (m, 1 H, C_5H_3), 4.49 (m, 1 H, C_5H_3), 4.31 (s, 5 H, C_5H_5), 3.61 (m, 1 H, C_5H_3), 2.32 (s, 3 H, Py *Me*), 2.12 (d, 3 H, CH*Me*N, J = 7). ^{13}C{^{1}H} NMR ($CDCl_3$): δ 151.2−126.6 (Ar *C*, Py *C*), 108.5 (Py *C*), 89.5 (d, C_5H_3, J = 16 Hz), 75.2 (C_5H_3), 74.7 (d, C_5H_3, J = 35), 71.2 (C_5H_5), 70.8 (d, C_5H_3, J = 4), 69.2 (d, C_5H_3, J = 5), 61.5 (*C*HMeN), 17.4, 12.6 (CH*Me*N, Py *Me*). ^{31}P{^{1}H} NMR (101.26 MHz, $CDCl_3$): δ 6.44 (PPh_2, J(P, Si)$_{trans}$ = 308 Hz). ^{29}Si NMR (99.4 MHz, $CDCl_3$): δ 19.3 (Si trans tro P, ^2J(Si_{trans},P) = 308); 14.3 (Si trans to N, ^2J(Si_{cis},P) = 11). Anal. Calcd for $C_{34}H_{31}N_2PFePdSi_2Cl_6$: C, 43.92; H, 3.36; N, 3.01. Found: C, 44.79; H, 3.57; N, 3.10.

Bis(trichlorosilyl)-{1-{(*R*)-1-[(*S*)-2-(diphenylphosphino-κ*P*)ferrocenyl]ethyl}-3-(2,4,6-trimethylphenyl)-1*H*-pyrazole-κ*N*}palladium (6). This compound was obtained from **3** (200 mg, 0.26 mmol) and $HSiCl_3$ (1 mL, 5.5 mmol) in CH_2Cl_2 (4 mL) by following the procedure described for **4**. The insoluble product precipitated upon standing at room temperature. The yellow crystals were filtered off, washed twice with hexane, and dried in vacuo. Yield: 216 mg, 86%. Some crystals were suited for X-ray diffractometry. Anal. Calcd for $C_{36}H_{35}N_2PFePdSi_2Cl_6$: C, 45.14; H, 3.68; N, 2.92. Found: C, 45.31; H, 3.84; N, 2.70.

Diiodo{1-{(*R*)-1-[(*S*)-2-(diphenylphosphino-κ*P*)ferrocenyl]ethyl}-3,5-dimethyl-1*H*-pyrazole-κ*N*}palladium (7). A mixture of **1** (50 mg, 0.075 mmol) and KI (45 mg, 0.298 mmol) was vigorously stirred in 2 mL of acetone. The color of the reaction mixture turned thereby from orange to dark red. The suspension was then filtered and the solvent evaporated in vacuo. Crystallization of the crude product from CH_2Cl_2/hexane gave a red microcrystalline material. Yield: 60 mg, 94%. Two different conformers could be identified by ^{31}P NMR spectroscopy in relative concentrations of 25:1. The minor conformer is ignored here, because of the incomplete spectroscopic signal attribution. Mp: >267 °C dec. ^{1}H NMR (250.131 MHz, $CDCl_3$): δ 7.79 (m, 2 H, Ph *H*), 7.56−7.24 (m, 5 H, Ph *H*, C*H*MeN), 7.19 (m, 2 H, Ph *H*), 6.87 (m, 2 H, Ph *H*), 5.34 (s, 1 H, Py *H*), 4.87 (m, 1 H, C_5H_3), 4.52 (m, 1 H, C_5H_3), 4.39 (s, 5 H, C_5H_5), 3.63 (m, 1 H, C_5H_3), 2.20 (s, 3 H, Py *Me*), 2.06 (d, 3 H, CH*Me*N, J = 7 Hz), 1.82 (s, 3 H, Py *Me*). ^{13}C{^{1}H} NMR (62.903 MHz, $CDCl_3$): δ 149.5−127 (Ph *C*, Py *C*), 110.7 (Py *C*), 90.7 (d, C_5H_3, J = 16 Hz), 74.9 (C_5H_3), 71.6 (d, C_5H_3, J = 50), 71.6 (C_5H_5), 70.8 (d, C_5H_3, J = 6), 68.6 (d, C_5H_3, J = 7), 58.2 (d, *C*HMeN, J = 2), 16.6, 15.9, 12.7 (Py *Me*, CH*Me*N). ^{31}P{^{1}H} NMR (101.259 MHz, $CDCl_3$): δ 16.1 (PPh_2, minor), 10.8 (PPh_2, major). FT-IR: 3139 w, 3078 w, 2988 w, 2917 w, 1812 w, 1553 s, 1480 m, 1465 w, 1454 w, 1435 s, 1397 m, 1371 s, 1328 s, 1266 w, 1244 m, 1218 w, 1165 m, 1106 s, 1095 s, 1075 w, 1058 w, 1042 m, 1001 m, 907 w, 853 m, 838 m, 822 m, 806 m, 752 m, 740 m, 696 s, 655 w, 619 w, 557 m, 513 s, 489 s, 468 s cm^{-1}. MS (FAB$^+$): *m*/*z* 852 ([M]$^+$, 2%), 725 ([M − I]$^+$, 100%), ([M − HI_2]$^+$, 20%). Anal. Calcd for $C_{29}H_{29}I_2FeN_2PPd$: C, 40.85; H, 3.43; N, 3.29. Found: C, 40.86, H, 3.46, N, 3.23.

X-ray Structure Analysis of 2, 5, and 6. Intensity data were collected at room temperature on a Siemens Platform CCD (charge coupled device) diffractometer. The program SMART (Siemens Analytical X-ray Systems Inc., Madison, WI) was used for the determination of the unit cell and for data collection. The data reduction was performed using SAINT (Siemens Analytical X-ray Systems Inc., Madison, WI). An empirical correction of the absorption was performed with SADABS (G. M. Sheldrick, University of Göttingen, Göttingen, Germany). The structures were solved and refined using the program SHELXS-96 (G. M. Sheldrick, SHELXS-96: Program for the Solution of Crystal Structures, University of Göttingen, Göttingen, Germany, 1996) by direct methods. There were two complex, two CH_2Cl_2, and two $CHCl_3$ molecules in the asymmetric unit of **2**. Each molecule of **5** was accompanied by 1 equiv of CH_2Cl_2. In complex **6** two chlorine atoms attached to the silicon atom Si(1) were found to be disordered between two positions (Cl(1)/Cl(1A) and Cl(2)/Cl(2A)). Refinement has been carried out with the occupancy factors f(Cl(1)) = f(Cl(1A)) = f(Cl(2)) = f(Cl(2A)) = 0.5, U(Cl(1)) = U(Cl(1A)), and U(Cl(2)) = U(Cl(2A)). One has to note that this situation does not apply to Cl(3) because of its relatively short nonbonding distances from Cl(5) and Cl(6) of 3.48 and 3.42 Å, respectively, constituting a steric constraint. Least-squares methods with anisotropic displacement parameters for all non-hydrogen atoms were used in the refinement of the complex molecules of all three compounds. However, the displacement parameters of the atoms in the solvent molecules and disordered atoms were left isotropic. All hydrogen atom positions were placed in calculated positions (riding model) with isotropic parameters, fixed at 1.5 times the U(eq) value of the carbon atom for the methyl groups and 1.2 times the U(eq) value of the carbon atom for all the other groups.

Acknowledgment. We thank Michael Wörle, Arianna Martelletti, and Diego Broggini for the X-ray crystallographic studies of **2**, **5**, and **6**. We also thank Heinz Rüegger for running the ^{31}P−^{29}Si{^{1}H}−HMQC experiment on compound **5**. G.P. is grateful to the Swiss National Science Foundation for financial support. T.K.W. wishes to thank the NSERC of Canada and the ETH for financial support.

Supporting Information Available: Tables of crystallographic parameters, atomic coordinates, all bond distances and angles, anisotropic displacement coefficients, and coordinates of hydrogen atoms for **2**, **5**, and **6**, an ORTEP representation with complete atom-numbering scheme for **2**, and tables of Cartesian coordinates for complex **6** (models **A**−**F**) and complex **5** (model **G**). This material is available free of charge via the Internet at http://pubs.acs.org. Tables of calculated and observed structure factors may be obtained from the authors upon request.

OM000130G